High-resolution spectroscopy of defect-bound excitons and acceptors in GaAs grown by molecular-beam epitaxy

M. S. Skolnick

Royal Signals and Radar Establishment, St. Andrews Road, Great Malvern, Worcestershire, United Kingdom

C. W. Tu and T. D. Harris

AT&T Bell Laboratories, 600 Mountain Avenue, Murray Hill, New Jersey 07974
(Received 25 July 1985)

New results on the groups of luminescence lines arising from defect-bound excitons and defect-complex acceptors in GaAs grown by molecular-beam epitaxy are reported. Both series of spectra are found to be polarized, thus establishing a strong link between them. Resonantly excited two-hole satellites of the defect-bound excitons are observed, supporting their identification as arising from exciton recombination at axial acceptor centers. Calculation of acceptor binding energies from the two-hole satellite displacements leads to reasonable agreement with those found from the electron to shallower defect-complex acceptor bands, providing a further clear connection between the two sets of bands.

I. INTRODUCTION

Künzel and Ploog first reported a series of bound exciton lines in the 1.504–1.511 eV spectral region in GaAs grown by molecular-beam epitaxy (MBE) in 1980.[1,2] Since that time a number of separate photoluminescence (PL) investigations have been published by several sets of authors including Briones and Collins,[3] Contour et al.,[4] Rao et al.,[5] and Skromme et al.[6] The highest-resolution spectra reported are those observed by Reynolds et al.[7] and Skolnick et al.,[8] with about fifty individual features being detected in the 7-meV energy range. One of the most striking effects, reported by Skolnick et al.[8] (also observed by Eaves and Halliday[9] and Weisbuch and Dingle[10]) is that most of the PL in this region is strongly polarized parallel to *one* of the $\langle 110 \rangle$ directions ($[\bar{1}10]$) in the (001) growth plane. This was attributed to preferential defect pair incorporation along the [110] direction, in preference to $[\bar{1}10]$, the two directions being distinguished on the surface monolayer during growth (for further discussion see Ref. 8). In the present context the term, defects, is taken to imply either intrinsic defects or contaminating impurities.

Further spectral features from 1.471 to 1.492 eV were observed by Briones and Collins[3] and studied more recently by Rao et al.[5] and Skromme et al.[6] Briones and Collins attributed the eleven lines they observed to electron recombination with a series of "defect-complex" acceptors. They also pointed out the possible relationship between these (e-A^0) transitions and the bound exciton lines in the 1.504–1.511 eV region. Eaves and Halliday[9] modeled the 1.504–1.511 eV lines as bound-exciton recombination at a series of acceptor pairs, with the high-energy limit corresponding to an isolated acceptor, and the low-energy limit to the nearest-neighbor acceptor pair. They pointed out that the total range of acceptor energies observed by Briones and Collins is consistent with the variation from an isolated acceptor to a nearest-neighbor, helium-like, double acceptor pair.

In the present paper new resonantly excited PL and PL excitation (PLE) measurements are presented which provide a firm link between the 1.504–1.511 eV and 1.47–1.48 eV structures. Strong supporting evidence for this conclusion is derived from the observation that the defect acceptor recombination also shows marked polarization effects.

The paper is organized in the following way. In the next section the experimental details are discussed. Then in Sec. III overall PL spectra, PL excitation, and resonantly excited PL spectra are presented and discussed, and then in Sec. IV the main conclusions of the paper are summarized.

II. EXPERIMENTAL

The experiments were carried out at 2 K principally on a 6-μm thick, very high purity sample (sample 1) of MBE GaAs. The layer was grown at 630 °C on a (001) growth plane with (2×4) surface reconstruction, in a Varian GEN2 machine. The nominally undoped sample is p type with residual acceptor concentration $\sim 10^{14}$ cm^{-3}. PL was excited with ~ 50 mW of tunable radiation from a Coherent Radiation jet-stream dye laser, containing Styryl 9 dye, pumped by 3–4 W of 5145-Å light from an argon-ion laser. The linewidth of the radiation from the dye laser was ~ 0.15 Å (0.03 meV). The PL was dispersed by a 0.85-m double spectrometer and detected with a thermoelectrically cooled GaAs photomultiplier tube.

III. RESULTS AND DISCUSSION
A. Photoluminescence spectra

In Fig. 1 the PL spectrum for the defect-bound exciton lines in the 1.504–1.511 eV spectral region, already published by Skolnick et al.,[8] is shown. It is repeated here since the details of the spectrum are essential for the
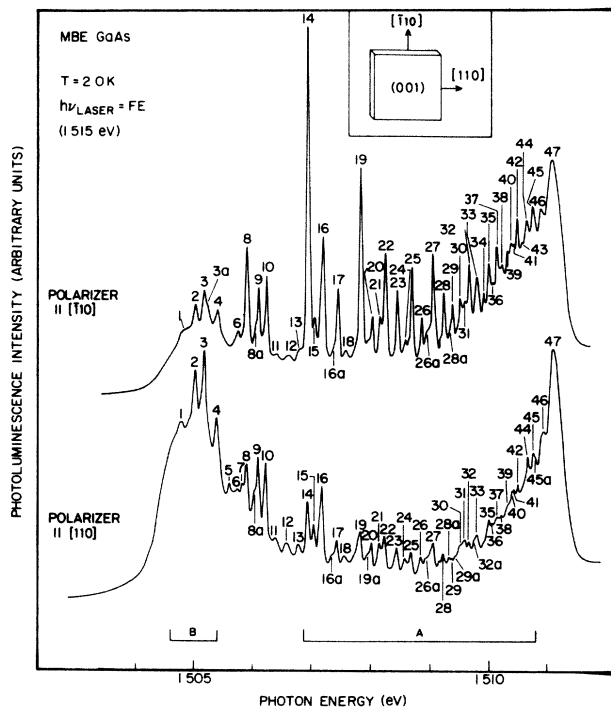
FIG. 1. Low-temperature (2 K) PL spectra for sample 1 excited with the dye laser set to the free-exciton energy at 1.515 eV. Spectra are shown for [110] and [$\bar{1}$10] polarizations. The A group of lines is polarized predominantly $||$ [$\bar{1}$10] and the B group $||$ [110]. The high-energy limit (47) is unpolarized as expected for distant pairs (see the text). The labeling of the peaks 1—47 is for reference purposes only, and does not imply any particular identifications. The inset shows a schematic diagram of the sample.

FIG. 2. "Defect-complex" electron to neutral acceptor transitions (e-A^0) labeled d_2,d_3,d_4 in the notation of Skromme et al., for [110] and [$\bar{1}$10] polarizations. The 4.2-K spectra are excited with the dye laser set to 1.67 eV.

comprehensibility of the following discussion. The spectrum is excited with the dye laser tuned to the free-exciton energy at 1.515 eV, to obtain maximum PL intensity. Spectra are shown for the polarizer in the detection system set parallel, successively, to the [110] and [$\bar{1}$10] directions in the (001) growth plane. As discussed by Skolnick et al.[8] the spectrum can be divided into two groups of lines, labeled A and B in Fig. 1. The prominent lines in the A group are polarized parallel to [$\bar{1}$10], whereas those in the B group are polarized in the perpendicular [110] direction. The polarization of the spectra is independent of the laser polarization for excitation at all energies above the defect-bound exciton lines. The A group of lines was attributed to σ dipole transitions resulting from bound-exciton recombination at defect pairs of varying separation oriented along [110], with the strongest line, 14, suggested to arise from the nearest-neighbor pairs. In the inset a schematic diagram of the (001) growth plane is shown with the two $\langle 110 \rangle$ directions marked.

To lower energy the electron-defect-complex acceptor peaks (e-A^0), first reported by Briones and Collins,[3] are observed, as shown in Fig. 2 for [110] and [$\bar{1}$10] polarizations. The term "defect-complex" acceptors is that employed by Briones and Collins. The peaks are labeled according to the notation of Skromme et al.[6] The spectrum
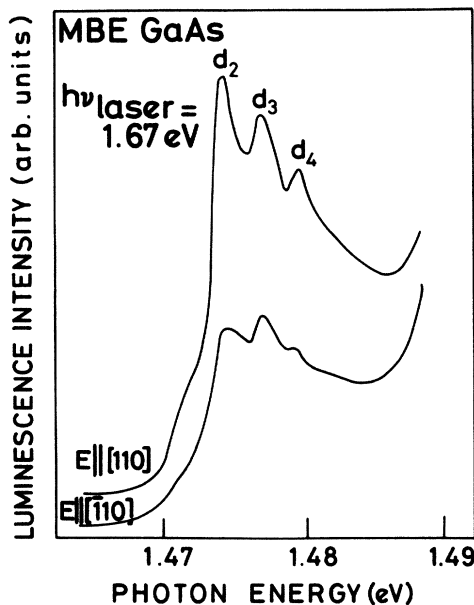
is excited with the dye laser set well above the band edge at 1.67 eV, since for near gap, nonresonant excitation very little intensity is obtained from peaks d_2—d_4 (see Fig. 4), perhaps because of the importance of competing bound exciton recombination paths under such conditions.

The d_2—d_4 lines occur below the (e-A^0) transition for the carbon acceptor at 1.493 eV. Carbon has been shown to be the dominant shallow acceptor in the sample from resonantly excited two-hole spectroscopy[11,12] of the shallow acceptor bound-exciton line (A^0,X) at 1.5123 eV. Skromme et al. have confirmed that the 1.47—1.48 eV peaks of Fig. 2 arise from (e-A^0) recombination.[6] They were able to observe the transition from donor-acceptor pair (D^0-A^0) to (e-A^0) as a function of increasing temperature in n-type samples, thus providing really good evidence for the attribution first proposed by Briones and Collins.[3]

The main new result of Fig. 2 is that the PL from the defect-complex (e-A^0) transitions also shows marked polarization, predominantly parallel to [110]. The observation of polarization provides additional support for a correlation between the polarized defect bound exciton lines of Fig. 1 and the (e-A^0) transitions of Fig. 2. In the same spectra the carbon (e-A^0) transitions at 1.493 eV are unpolarized (not shown). The polarization effects for the d_2, d_3, and d_4 (e-A^0) transitions imply that the acceptors taking part in the recombination must have strong axial symmetry, with preferential incorporation along the $\langle 110 \rangle$-type directions.

B. Photoluminescence excitation spectra

High-resolution PLE spectra with the dye laser scanned through the 1.503—1.513 bound-exciton region are shown in Fig. 3. The spectrometer detection is set to 1.4686 eV,
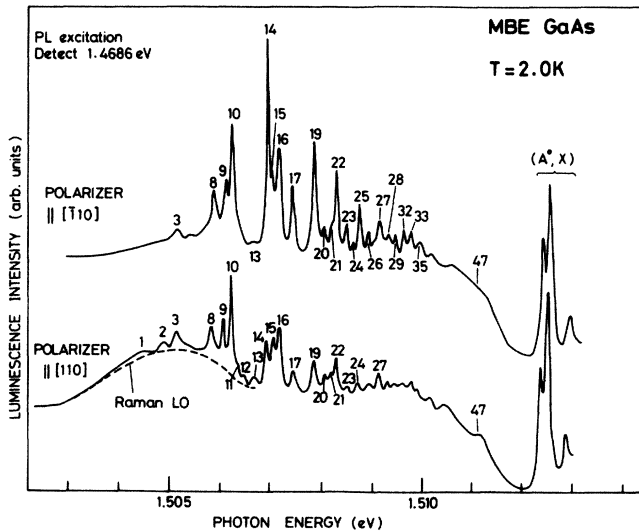
FIG. 3. PL excitation spectra, at 2 K, recorded through the defect-bound-exciton region from 1.504 to 1.511 eV. The spectrometer detection is set at 1.4686 eV (2-meV bandpass), corresponding to the peak labeled S in Fig. 4. At high energy the carbon (A^0,X) transitions are visible as positive features in the PLE spectra. Spectra are shown for [110] and [$\bar{1}$10] polarizations. The A group of lines 14 to ~35 show the same polarization and relative intensities as the PL spectra of Fig. 1. The broad structure underlying the B group of lines (1—4) in Fig. 1 is not present in the PLE spectra.

with very wide slits being employed to give a detection bandpass of ~2 meV. Spectra are shown for [$\bar{1}$10] and [110] polarizations, in this case the polarization being that of the laser beam used for excitation. No deliberate polarization discrimination is employed in the detection system, although the uncorrected spectrometer response favors [110] polarization over [$\bar{1}$10] by a factor of about 4 to 1.

The most important result of Fig. 3 is that all the sharp PL lines from 1 up to at least 35 (notation of Fig. 1) are observed in PLE. The lines from 14 to 35 (the A group) have very similar relative intensities to those found in PL. Taken together with the result that no thermalization between the sharp lines was observed in PL spectra from 2 to 20 K,[8] nor in PLE from 2 to 4.2 K, it can be deduced that all the bound-exciton lines (at least in the A group) are transitions from the lowest state of the bound exciton to the ground state of the defect, and that each line observed arises from a transition at an independent center.

The series limit, line 47, which may correspond to distant pairs, is very weak in PLE, even if the detection is shifted to higher energy, possibly implying that line 47 has a separate origin from the rest of the bound exciton series. It should be noted that 47 is also observed in GaAs grown by liquid phase epitaxy[1] or metal-organic chemical vapor deposition.[8]

The other notable result is that the same polarization effects are observed in the absorption processes giving rise to the PLE spectra, as are found in the PL of Fig. 1. The broad structure underlying peaks 1—3 for [110] polarization, drawn as a dashed line in Fig. 3, arises from LO

phonon Raman scattering processes ($\omega_{LO}=36.7$ meV),[13] the large linewidth reflecting the very low spectrometer resolution of ~2 meV. The spectra of Fig. 3 demonstrate that although the PL from these MBE samples is independent of laser polarization for excitation at the carbon (A^0,X) line and above, this is not true for resonant excitation in the defect-bound exciton region. There is a strict polarization selection rule for the defect-bound exciton transitions whether observed in PL or absorption (i.e., PLE).

The almost complete absence in PLE of the broad feature underlying lines 1—4 observed in PL (labeled S_0 in Ref. 8) is believed to indicate that this structure arises from a final-state splitting in the PL experiment (initial state in PLE), the upper levels giving rise to this feature not being populated at the low temperatures employed for Fig. 3. The absence of the broad feature in PLE is demonstrated more clearly in experiments where the detection energy is changed so that the Raman line moves out of this range, leaving the 1—4 region unobscured. In these circumstances, a broad underlying feature is not observed with any significant intensity. It may be that each strong line in the 14, 16, 19, 22, etc., series has a broad low-energy satellite in the 1—4 region, the extra width perhaps arising from strong phonon-induced relaxation from the excited states to the ground levels involved in 14, 16, etc. This tentative conclusion is supported by resonantly excited PL experiments, where direct excitation into 14, 16, etc., gives rise to a broad satellite in the 1—4 region.[14] At the same time such experiments demonstrate that 1—4 themselves are not satellites of 14, 16, etc.

C. Resonantly excited photoluminescence

The PLE spectra of Fig. 3 are only obtained for detection in the 1.468—1.470 eV spectral region. It is clear that spectral features related to the defect-bound exciton lines are being detected in this region. However, the actual PL feature detected is a strong function of the energy of the exciting laser. For this reason, no definite statements about what spectral features were being monitored were made in the previous section.

PL spectra in the 1.450—1.480 eV region for a number of different excitation energies are shown in Fig. 4. In Fig. 4(a) the dye laser is set above the band edge at 1.526 eV, and in Fig. 4(b) it is resonant with the free exciton at 1.5148 eV. The feature labeled S, obtained under these conditions, occurs at 1.4686 eV, the detection energy employed for the PLE spectra of Fig. 3. It occurs at one LO phonon energy (36.7 meV) below the broad feature (S_0 in Ref. 8) underlying 1—4. Thus, S may well be an LO phonon replica, although similar satellites of the defect-bound exciton lines themselves could not be positively identified. Support to this attribution is given by the observation that very similar PLE spectra to those of Fig. 3 in the region 14—47, are obtained for detection of S_0 directly at 1.5047 eV.

As the dye laser position is brought to lower energy [Figs. 4(c)—4(h)] to be resonant with the various PLE peaks of Fig. 3, a number of sharp satellites are observed in the PL spectra, labeled X, P, Q, T, etc. All the results are summarized in Fig. 5, where the energies of the satellites below the laser line are plotted as a function of laser
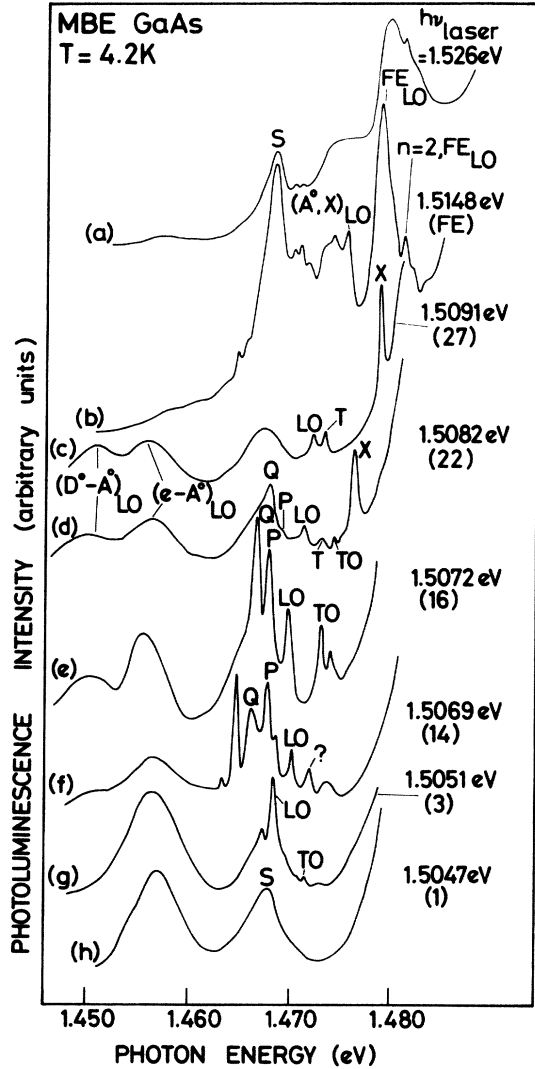
FIG. 4. Selectively excited PL spectra in (c)—(h) with the laser tuned successively to be in resonance with sharp peaks in the PLE spectra of Fig. 3. Traces (a) and (b) are for above gap and free-exciton excitation, respectively. The $(D^0\text{-}A^0)$ and $(e\text{-}A^0)$ bands from 1.45—1.46 eV are due to carbon acceptors. The PLE spectra of Fig. 3 are taken with the spectrometer detection on peak S of (a), (b), and (h). The peak labeled X is identified as a resonantly excited two-hole satellite of the defect-induced bound-exciton lines.
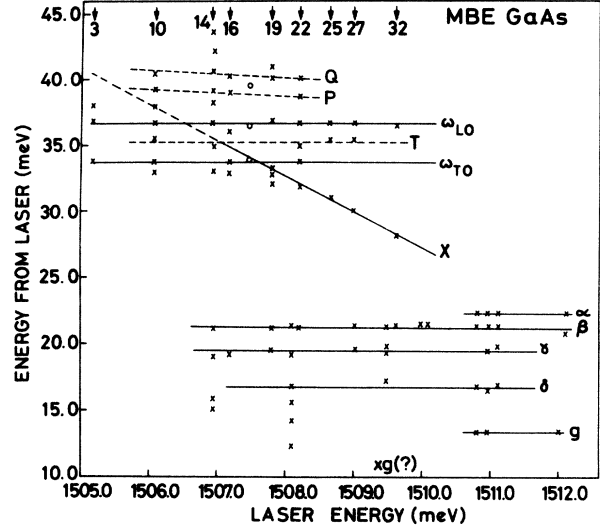

FIG. 5. Summary of the results of Fig. 4 in the 25—45 meV region. The vertical axis is the energy displacement below the exciting laser energy, while the horizontal axis gives the actual laser energy. The crosses in the upper part of the figure signify observed peak positions for a series of resonant excitation energies, while the open circles correspond to nonresonant excitation between lines 16 and 19. The lower part of the figure (10—23 meV satellites from the laser energy) summarizes the results shown in Fig. 6. Most of these peaks can be identified as selectively excited carbon acceptor-donor pair luminescence. For more details see the text.

excitation energy. All experimental points are included on this figure, although spectra for all excitation energies are not given on Fig. 4 for purposes of clarity.

The Raman lines (ω_{LO} and ω_{TO} in Fig. 5) occur at a constant separation from the laser line. The line labeled X, observed only when the laser is in resonance with one of the defect-bound exciton lines, (the actual laser resonance positions are marked along the top of the figure) increases in separation from the laser line as the laser is tuned in the direction of lower energy, in the sense of 32, 27, 25, etc. This is just the behavior expected if the X lines are the "two-hole" satellites[11,12] of each of the individual defect-bound excitons in turn. This attribution implies that the bound-exciton lines correspond to exciton

recombination at neutral acceptor centers, as already suggested in previous sections, where the acceptor is left in its $1s$ ground state after recombination. The two-hole satellites (X) correspond to recombination where the acceptor is left in a $2s_{3/2}$ excited state, (equivalent to a resonant electronic Raman scattering process) the separation between the two lines (the ordinate on Fig. 5) being the $1s_{3/2}\text{-}2s_{3/2}$ energy of the neutral acceptor. Use of the 3/2 subscript to describe the $1s,2s$ acceptor stares is not strictly correct[15] since the degeneracy of the 3/2 angular momentum state of the valence-band maximum will be lifted in the axial field of the defect acceptors (see end of Sec. III A). For this reason, in the discussion that follows the 3/2 subscript will be omitted.

From the observed $1s\text{-}2s$ energies ($E^{obs}_{1s\text{-}2s}$), the binding energies of the acceptors can be estimated, assuming that the $2s$ state has one eighth the chemical shift of the $1s$ state, and that the effective mass $1s\text{-}2s$ separation ($E^{EM}_{1s\text{-}2s}$) is 18.4 meV for acceptors in GaAs.[15] The results are given in Table I for resonant excitation into lines 32, 27, 25, 22, and 19 using the following expression:

$$E^{EM}_{1s\text{-}2s} + \frac{7\Delta}{8} = E^{obs}_{1s\text{-}2s} \tag{1}$$

and

$$E_B = E^{EM}_B + \Delta , \tag{2}$$

where $E^{EM}_B = 25.4$ meV is the effective-mass acceptor binding energy and Δ is the central cell correction (chemi-

TABLE I. Results for resonant excitation.

Line number	Bound exciton energy (meV)	$1s$-$2s$ satellite energy[a] (meV)	Acceptor binding energy (meV)
32	1509.62	28.1	36.5
27	1509.10	30.0	38.7
25	1508.66	31.0	39.8
22	1508.22	31.8	40.7
19	1507.80	33.2	42.3
22–25		31.3[b]	40.1 (d_4)
16–19[c]		34.4[b]	43.7 (d_3)
12–14[c]		36.3[b]	45.8 (d_2)
8–10[c]		38.1[b]	47.9 (d_1)

[a]Assuming X satellites of Figs. 4 and 5 arise from two-hole satellites of lines 32–19.
[b]Calculated from the results of Skromme et al. quoted in the last four lines of the third column of the table.
[c]Correlations with d_1 to d_4 acceptors deduced from extrapolation of the Haynes's rule plot of Fig. 6 to the region below line 19.

cal shift) of the $1s$ ground state. Values for the acceptor binding energies ranging from 36.5 to 42.3 meV are obtained. These compare very well with the lower range of the binding energies for acceptors d_4–d_1 obtained by Skromme et al. of 40.1–47.9 meV,[6] particularly considering that no account has been taken of the perturbation of these levels by the axial fields at the acceptors.

The good agreement between the acceptor binding energies obtained by two completely independent techniques provides strong support for the identification for the X lines as two-hole satellites, and of the 1.507–1.511 eV peaks as acceptor bound-exciton lines. The observation of such satellites which arise from a splitting in the final state of the transition excludes the possibility that the excitons are bound to isoelectronic centers where there are no free electronic particles at the center after exciton recombination.

For excitation below line 22, the satellite structure becomes more complicated (for 19, 16, 14, 10 excitation), and it is not easy to follow the X line. The circles in Fig. 5, for excitation between 16 and 19, indicate that the complicated structure is not obtained for nonresonant excitation. The structure to higher energy than ω_{LO} may arise from local phonon satellites, associated with vibrations at the particular defect centers, or from transitions to more highly excited states of the acceptors, or possibly may be due to interparticle interactions for the closer pairs. On the double acceptor model of Eaves et al., an additional splitting of the X two-hole satellites due to hole-hole interaction would be expected. For resonant excitation down to line 22 no such splitting is observed. One possible reason for this could be that the splitting is too small to be observed for relatively distant pairs since the hole-hole overlap will be small. For closer pairs (19, 14, etc.) the additional structure observed may be indicative of hole-hole interactions. However, it should be emphasized that the data presented here give strong evidence for the involvement of one acceptor in the complexes. No direct information is obtained for the role of a second acceptor in the oriented pairs.

The results of Table I and Fig. 5 are plotted in the form of a "Haynes's rule" plot[16] of exciton localization energy (E_x) against acceptor binding energy (E_B) in Fig. 6. The

exciton localization energies are the energy difference between the transverse free-exciton energy of 1.515 eV (Ref. 17) and the bound-exciton energies. The approximate straight-line behavior found in Fig. 6 shows that Haynes's rule, which predicts a linear dependence of exciton localization energy on acceptor binding energy, is reasonably well obeyed by the defect-bound exciton-defect complex acceptor systems. The same dependence is demonstrated by the linear variation of the X satellite displacement energies (the acceptor $1s$-$2s$ energies) against bound-exciton energy in Fig. 5.

It should be noted that Haynes's rule does not hold for the common chemical substituent acceptors in GaAs (e.g., C, Zn, Cd) where the exciton localization energy is insensitive to variations in the acceptor binding energy.[12,18] The applicability of Haynes's rule for the defect centers may simply be an expression of the fact that each line (in the
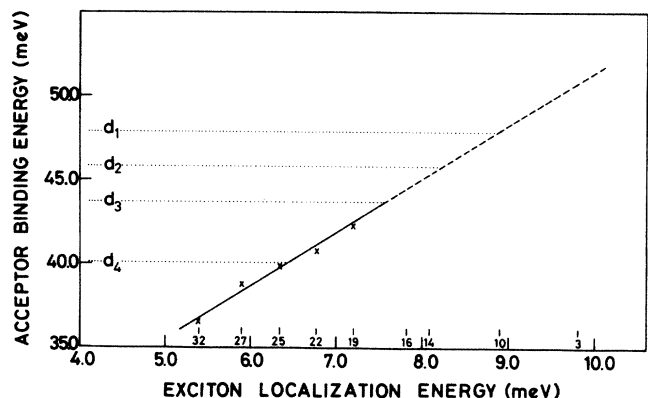

FIG. 6. "Haynes's rule" plot of acceptor binding energy calculated using Eqs. (1) and (2) from results of Fig. 5. The reasonably straight-line behavior demonstrates that Haynes's rule is obeyed for the defect-bound exciton-defect acceptor system. The same basic information can be obtained from the X-satellite displacements ($1s$-$2s$ acceptor energies) plotted against exciton energy in Fig. 5, where a straight-line variation is also obtained. The energies of the d_1–d_4 acceptors from Ref. 6 are indicated by horizontal lines. The defect-bound-exciton energies are given on the horizontal axis.

range 32—19 at least) is a slightly perturbed form of the same basic center. In the model described in the Introduction this is expected since in the sequence 32—19, successively closer pairs of the same two centers are involved in the recombination. A value for $\Delta E_x/\Delta E_B$ of 0.33 ± 0.05 is obtained from Table I and Fig. 6, and is in fairly good agreement with that obtained earlier by Briones and Collins of 0.38,[3] but without the detailed spectroscopic proof given in the present paper.

The energies of the defect acceptors (d_1 to d_4) observed by Skromme et al.[6] and shown in Fig. 3 have been represented by horizontal lines in Fig. 6. From Fig. 6, d_4 is found to correspond to bound excitons 22—25, d_3 to 16—19, d_2 to 12—14, and d_1 to 8—10. These results are also summarized in the last four lines of Table I, where the X satellite energies for d_1-d_4 calculated from Eq. (1) are also given. It should be noted that the above bound exciton-acceptor correspondences should not be taken too precisely since clearly a lot more structure is observed in the bound exciton than in the (e-A^0) region, but the general method employed to obtain the connections should be reliable. The resolution of the peaks in the (e-A^0) region is limited to about 1.5 meV by the intrinsic linewidth of these transitions, as opposed to the 0.04-meV linewidth for the bound exciton lines. Further difficulties in obtaining reliable correspondences between the bound excitons and acceptors arise because several resonantly excited satellites of the bound excitons occur for excitation at energies lower than line 22. This is just the region needed to predict which bound excitons arise from d_1-d_4. In addition within the limits quoted for the ratio $\Delta E_x/\Delta E_B$ $=0.33\pm0.05$, the d_1 acceptor could also just be identified with the 1—4 exciton region.

The spectra for the lower-energy satellite (10—23 meV) region of Fig. 5 are shown in Fig. 7. Most of the observed features can be ascribed to selectively excited pair luminescence of carbon acceptor-donor pairs. In these processes, previously reported for acceptors in GaAs by Hunter and McGill[19] and Kisker et al.,[20] a donor-acceptor pair at a particular separation is neutralized with the hole being raised to an excited state of the acceptor. The detected recombination occurs between donor and acceptor ground states. These processes have been discussed in detail by Tews et al.[21] By comparison with the published literature, peaks α (22.3 meV separation from the laser), β (21.1 meV), and γ (19.5 meV) can be identified as arising from excitation transitions to the $3s_{3/2}$, $2p_{5/2}(\Gamma_7)$, and $2p_{5/2}(\Gamma_8)$ states of the carbon acceptor.[20] These are the best-defined peaks in the spectra of Fig. 7. The identification of the weak shoulders (δ at 16.8 meV, g at $\sim$13.5 meV) is less clear. δ occurs between the expected positions for $2s_{3/2}$ (18.4 meV) and $2p_{3/2}$ (15.2 meV) features. The lowest-energy feature has been labeled g, following the work of Contour et al.[4] who observed a resonantly enhanced feature at 15.5 meV below the laser line for excitation in the region of the series limit (line 47 at 1.511 eV). These authors ascribed the g line to a two-hole satellite of the bound-exciton transition at 1.511 eV. However, we have not been able to reproduce this clearly in our samples, although there are some weak, poorly resolved lower-energy satellites in this region plotted in Fig. 5.

Contour et al.[4] did not report any of the richly structured, lower-energy structure of Fig. 4.

There does not appear to be any selectively excited pair luminescence for the d_2-d_4 acceptors in Figs. 4 and 5. This is probably because the spectra are taken under resonant conditions which favor competing bound-exciton recombination.
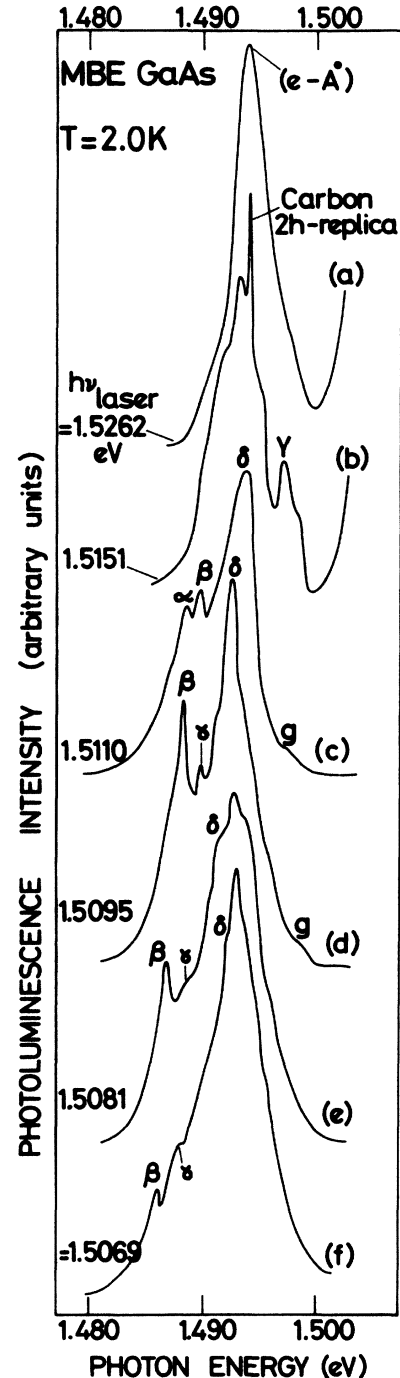

FIG. 7. Selectively excited PL spectra in the carbon (e-A^0) region (results plotted in lower half of Fig. 5). Curve (a) is for above gap excitation, (b) for free-exciton excitation, and (c)—(f) for energies within the defect-bound-exciton region. For discussion see the text.

IV. CONCLUSIONS

The data presented in this paper represent some significant steps forward in the understanding of the defect bound exciton lines, and the defect-complex acceptor $(e\text{-}A^0)$ transitions in MBE GaAs. The observation of polarization of the PL for both sets of recombination bands provides a strong link between them. In addition, the attribution of low-energy satellites of the bound-exciton lines to two-hole transitions permits the calculation of acceptor binding energies in good agreement with those obtained from the upper energy range of the $(e\text{-}A^0)$ transitions, and leads to the conclusion that the defect-bound-exciton lines arise from recombination at a series of neutral acceptors.

In spite of the new results presented here, a number of unresolved problems still remain in the analysis of these spectra. The major difficulty is the identification of the impurity species (if any) involved in these centers. In this context the possible evidence for the role of carbonyl molecules, presented by Akimoto et al.[22] is noteworthy. The other important problem is to obtain a reliable fitting to the line positions of the spectra of Fig. 1. This has been attempted by Eaves and Halliday on much less-well-resolved spectra.[9] However, their fitting took no account of the polarization and the restrictions this implies as to the possible pair orientations.[8] The deduction of the detailed systematics of the variations between the series of centers remains a difficult task. However, this is being attempted at the present time with the aid of the results of Zeeman spectroscopic investigations.

ACKNOWLEDGMENTS

[1]H. Künzel and K. Ploog, Appl. Phys. Lett. 37, 416 (1980).

[2]H. Künzel and K. Ploog, GaAs and Related Compounds, Vienna, 1980, edited by H. W. Thim (Institute of Physics, London, 1981), p. 519.

[3]F. Briones and D. M. Collins, J. Electron. Mater. 11, 847 (1982).

[4]J. P. Contour, G. Neu, M. Leroux, C. Chaix, B. Levesque, and B. Etienne, J. Vac. Sci. Technol. B 1, 811 (1983).

[5]E. V. K. Rao, F. Alexandre, J. M. Masson, M. Allovon, and L. Goldstein, J. Appl. Phys. 57, 503 (1985).

[6]B. J. Skromme, S. S. Bose, B. Lee, T. S. Low, T. R. Lepkowski, R. Y. DeJule, G. E. Stillman, and J. C. M. Hwang, J. Appl. Phys. 58, 4685 (1985).

[7]D. C. Reynolds, K. K. Bajaj, C. W. Litton, E. B. Smith, P. W. Yu, W. T. Masselink, F. Fisher, and H. Morkoc, Solid State Commun. 52, 685 (1984).

[8]M. S. Skolnick, T. D. Harris, C. W. Tu, T. M. Brennan, and M. D. Sturge, Appl. Phys. Lett. 46, 427 (1985).

[9]L. Eaves and D. P. Halliday, J. Phys. C 17, L705 (1984); D. P. Halliday, L. Eaves, and P. Dawson, Proceedings of the 13th International Conference on Defects in Semiconductors, Transactions of the Metallurgical Society, Coronado, 1984 (AIME, New York, 1985), Vol. 149, p. 1005.

[10]C. Weisbuch and R. Dingle (private communication).

[11]P. J. Dean, J. D. Cuthbert, D. G. Thomas, and R. T. Lynch, Phys. Rev. Lett. 18, 122 (1967).

[12]D. J. Ashen, P. J. Dean, D. T. J. Hurle, J. B. Mullin, and A. M. White, J. Phys. Chem. Solids 36, 1041 (1975).

[13]A. Mooradian and G. B. Wright, Solid State Commun. 4, 431 (1966).

[14]T. D. Harris and M. S. Skolnick (unpublished).

[15]See, for example, A. Baldereschi and N. O. Lipari, Phys. Rev. B 9, 1525 (1974) for explanation of notation and discussion of shallow acceptor states in T_d symmetry.

[16]J. R. Haynes, Phys. Rev. Lett. 4, 361 (1960).

[17]R. G. Ulbrich and C. Weisbuch, Phys. Rev. Lett. 38, 865 (1978).

[18]P. J. Dean and D. C. Herbert, in Excitons, edited by K. Cho (Springer-Verlag, Berlin, 1979), p. 55.

[19]A. T. Hunter and T. C. McGill, Appl. Phys. Lett. 40, 169 (1982).

[20]D. W. Kisker, H. Tews, and W. Rehm, J. Appl. Phys. 54, 1332 (1983).

[21]H. Tews, H. Venghaus, and P. J. Dean, Phys. Rev. B 19, 5178 (1979).

[22]K. Akimoto, M. Donsen, M. Arai, and N. Watanabe, J. Vac. Sci. Technol. B 3, 622 (1985).